European Review for Medical and Pharmacological Sciences 2019; 23 (3 Suppl): 47-53

Repair of spinal cord injury in rats by umbilical cord mesenchymal stem cells through P38MAPK signaling pathway

D.-Z. TIAN[1], D. DENG[2], J.-L. QIANG[1], Q. ZHU[1], Q.-C. LI[1], Z.-G. YI[1]

[1]Department of Neurosurgery, Cardiovascular Specialist Units, Affiliated Hospital of Yanan University, Yan'an, Shaanxi, China
[2]Department of Neurology, Daqing Oilfield General Hospital, Daqing, Heilongjiang, China

Dezhou Tian and *Dan Deng* contributed equally to this work

Abstract. – OBJECTIVE: To explore the repair of spinal cord injury (SCI) in rats by umbilical cord mesenchymal stem cells (UCMSCs) through the p38mitogen-activated protein kinase (MAPK) signaling pathway.

MATERIALS AND METHODS: A total of 45 healthy adult male Sprague-Dawley rats weighing 180-220 g and aged 6-8 weeks old were randomly divided into group A (SCI model + transplantation of UCMSCs, n=15), group B (sham operation), and group C (SCI model + injection of an equal dose of DMEM, n=15) using a random number table. The morphology of spinal cord tissues was observed via hematoxylin-eosin (HE) staining, and the protein expression of phosphorylated p38 (p-p38) in spinal cord tissues, the expression of glial fibrillary acidic protein (GFAP) in the injury region, and the spinal cord neuronal apoptosis were detected via Western blotting, immunofluorescence labeling and terminal deoxynucleotidyl transferase-mediated dUTP nick end labeling (TUNEL) assay, respectively.

RESULTS: In group B, there was no significant damage to the structure of spinal cord tissues. In group C, the spinal cord tissues had a disordered structure and significant fragmentation, the damage to grey matter was the greatest. Also, almost all of the grey matter was destroyed and dissolved, with a large number of scars and cavitation, and it was hard to distinguish the gray matter and white matter. In group A, the spinal cord tissues had a clear structure, there were smaller necrotic cavitation regions in the grey-white matter, and the number of cavitation significantly declined compared with that in group C. The results of immunofluorescence assay revealed that the expression of GFAP in spinal cord tissues was the lowest in group B, while it was remarkably decreased in group A compared with that in group C ($p<0.05$), suggesting that injecting UCMSCs via the caudal vein can prominently reduce the expression of GFAP in spinal cord tissues. Moreover, the spinal cord neuronal apoptosis rate was (4.21±0.19), (0.72±0.21) and (4.57±0.31), respectively, in group A, group B, and group C. It can be seen that the spinal cord neuronal apoptosis rate significantly declined in group A due to the treatment with UCMSCs. Also, the significant difference compared with that in group C, while it was significantly increased in group A compared with that in group B, but lower than group C ($p<0.05$). According to the results of Western blotting, the protein expression of p-p38 in spinal cord tissues was remarkably decreased in group B compared with that in group A and group C ($p<0.05$), while it was also markedly decreased in group A compared with that in group C ($p<0.05$), indicating that injecting UCMSCs via the caudal vein can significantly lower the protein expression of p-p38 in spinal cord tissues.

CONCLUSIONS: UCMSCs promote the recovery of neurological function, inhibit the p38 MAPK pathway activated after SCI, and reduce the spinal cord neuronal apoptosis in SCI rats.

Key Words:
Spinal cord injury, p38 MAPK, GFAP, Umbilical cord mesenchymal stem cells.

Introduction

Spinal cord injury (SCI) is a complication after an injury of the spine, with extremely high fatality and disability rates. There are two types, secondary and primary injury, both of which are caused by external forces[1,2]. Mesenchymal stem cells (MSCs) have a certain effect on SCI, which

Corresponding Author: Qiang Zhu, BM; e-mail: zhuq968@163.com

can be extracted and cultured in many human tissues. One of the treatments means for SCI is the stem cell transplantation. It has been reported[3,4] that the proliferation and differentiation ability of stem cells will decline with the aging of patients. MSCs can be cultured from many human tissues, the proliferation rate of which, however, is far lower than that of umbilical cord MSCs (UCMSCs). Therefore, UCMSCs have greater development prospect in stem cell transplantation. The effects of UCMSCs on the repair and regeneration of nerve tissues have attracted increasingly more attention in scientific research. It is reported[5,6] that the stem cell differentiation and proliferation in the tumor microenvironment is one of the important reasons for the enhanced tumor growth. Also, the cell proliferation and differentiation are also the basic attributes during the evolution of organisms. The mitogen-activated protein kinase (MAPK) signaling pathway is one of the important signaling pathways for the proliferation and differentiation of bone marrow MSCs into osteoblasts[7,8], including extracellular signal-regulated kinase (ERK)1/2 and p38 MAPK. Osteoblast differentiation is mainly realized through the p38 MAPK pathway[9,10]. Some studies[11] have demonstrated that the neuronal apoptosis is caused by the signal transduction, during which p38 MAPK plays an important role. Also, p38 MAPK can reflect the degrees of neuronal apoptosis and proliferation and tissue injury. Therefore, the SCI model was established for comparison in the present study, and the effect of UCMSCs on the repair of SCI in rats through the p38MAPK signaling pathway was explored.

Materials and Methods

Main Reagents and Instruments

Phosphorylated p38 (p-p38) MAPK monoclonal antibody (Wuhan D.A Biotechnology Co., Ltd., Wuhan, China), goat anti-rabbit immunoglobulin G (IgG; SLB, Beijing), terminal deoxynucleotidyl transferase-mediated dUTP nick end labeling (TUNEL) apoptosis assay kit (KG, Jiangsu, Nanjing, China), fluorescence microscope (Beijing Keyu Technology Co., Ltd., Beijing, China), and UCMSCs (Shandong Human Umbilical Cord Mesenchymal Stem Cell Bank, Heze, China).

Culture of UCMSCs

UCMSCs were cultured in the Dulbecco's Modified Eagle's Medium (DMEM; Hyclone, South Logan, UT, USA) containing 5% fetal bovine serum (FBS; Hyclone, South Logan, UT, USA) in an incubator with 5% CO_2 at 37°C. After the first passage, UCMSCs were passaged for multiplication culture at a ratio of 1:3 every 3 days. After culture for 8-10 d, the cells were used for experiments.

Animal Modeling and Transplantation of UCMSCs

The SCI model was established according to the methods in literature, briefly as follows: rats were anesthetized *via* intraperitoneal injection of chloral hydrate (0.33 mL/kg) and fixed on the plate, followed by standard T9-10 laminectomy. Then, the spinal cord was exposed in an aseptic environment, and the T9-10 spine was impacted using an impact device (height: 25 mm, weight: 10 g, diameter: 2 mm) to induce the paralysis of the hind limb. After SCI, the spinal cord was washed with normal saline. First, the incision was sutured and penicillin (80,000 U/0.1 mL) was intraperitoneally injected for 3 consecutive days. Next, the bladder was pressed every day to help urinate until the normal urinary function was reconstructed. At 6 d after successful modeling, 1 mL of UCMSC suspension (3×10^6/L) was injected *via* the caudal vein. At 4 weeks after successful modeling, the Basso-Beattie-Bresnahan (BBB) score was given. Then, the rats were sacrificed *via* cervical dislocation, and the spine specimens were collected. This research was approved by the Animal Ethics Committee of Yanan University Animal Center.

Laboratory Animals and Grouping

A total of 45 healthy adult male Sprague-Dawley rats weighing 180-220 g and aged 6-8 weeks old were provided by Shandong Laboratory Animal Center, and fed in separate cages in the specific pathogen-free animal room under the room temperature of (22±2)°C, humidity of 50-60% and 12/12 h light/dark cycle. Also, they had free access to food and water. The rats were randomly divided into group A (SCI model + transplantation of UCMSCs, n=15), group B (sham operation), and group C (SCI model + injection of an equal dose of DMEM, n=15) using a random number table.

Observation of Morphology of Spinal Cord Tissues Via Hematoxylin-Eosin (HE) Staining

The rats were sacrificed *via* dislocation at one time. The spinal cord tissues were isolated

and treated with 4% paraformaldehyde/phosphate-buffered saline (PBS) (pH 7.4) at 4°C for 48 h. The tissues were washed with running water, dehydrated with 70%, 80%, and 95% ethanol, and treated with 100% ethanol. The ethanol was removed with xylene. Then, the tissues were embedded into paraffin (4 μm in thickness) and stained in strict accordance with the manufacturer's instructions of the HE staining kit (Beyotime, Shanghai, China).

Detection of p38 Expression in Tissues Via Western Blotting

An appropriate amount of radioimmunoprecipitation assay (RIPA) lysis buffer was prepared, and the protease inhibitor phenylmethanesulfonyl fluoride (PMSF) (RIPA:PMSF = 100:1) (Beyotime, Shanghai, China) was added and mixed evenly. The spinal cord tissues were cut into pieces, added with tissue lysis buffer at a ratio of 10:1 and transferred into an Eppendorf (EP) tube, followed by centrifugation at 14000 rpm and 4°C for 30 min using the refrigerated high-speed centrifuge. Then, the protein supernatant was collected and subjected to a heating bath at 95°C for 10 min for protein denaturation. The protein samples prepared were stored in a refrigerator at –80°C for later use, and the protein was quantified using the bicinchoninic acid (BCA) kit (Pierce, Rockford, IL, USA). After that, the dodecyl sulfate, sodium salt-polyacrylamide gel electrophoresis (SDS-PAGE) gel was prepared, and the protein samples were loaded into the gel loading well for electrophoresis under the constant voltage of 80 V for 2.5 h. Then, the protein was transferred onto a polyvinylidene difluoride (PVDF) membrane (Millipore, Billerica, MA, USA) using a semi-dry transfer method. The PVDF membrane was immersed in Tris-Buffered Saline and Tween-20 (TBST) containing 5% skim milk powder and shaken slowly for 1 h on a shaking table to be sealed. Then, the protein was incubated with the primary antibody diluted with 5% skim milk powder, rinsed with TBST for 3 times (10 min/time), incubated again with the secondary antibody at room temperature for 2 h, and rinsed again with TBST twice and with TBS once (10 min/time). Finally, the protein was detected using the enhanced chemiluminescence (ECL) reagent, followed by exposure in a dark room. The relative expression of the protein was analyzed using Image-Pro Plus v6 (Media Cybernetics, Silver Spring, MD, USA).

Detection of Glial Fibrillary Acidic Protein (GFAP) Expression in the Injury Region Via Immunofluorescence Labeling

The target spinal cord was exposed through the original surgical incision in modeling, and the T10-centered spinal cord tissue specimens (1.5 cm) were taken. The 4 μm-thick frozen sections were rapidly prepared, followed by immunofluorescence observation, and washed with PBS for 3 times (10 min/time). After 0.05% Triton-100 was added to rupture the cell membrane, the sections were sealed with 3% goat serum at room temperature for 30 min, incubated with the GFAP primary antibody (1:100) in a wet box at 4°C overnight, washed with PBS for 3 times (10 min/time), incubated again with the secondary antibody (1:1000) in a dark place at room temperature for 1 h, and washed again with PBS for 3 times (10 min/time). The excess water on the glass slide was sucked dry using the filter paper, and one drop of buffered glycerin was added to avoid drying specimens. Finally, the sections were covered with the cover glass, and immediately observed under a fluorescence microscope.

Detection of Spinal Cord Neuronal Apoptosis Via TUNEL Assay

4 μm-thick paraffin sections were prepared and deparaffinized with xylene for 5-10 min. Next, the sections were deparaffinized again with fresh xylene for 5-10 min, treated with absolute ethanol for 5 min, 90% ethanol for 2 min, 70% ethanol for 2 min, distilled water for 2 min. Then, DNase-free proteinase K (20 μg/mL) was added dropwise. Then, the proteinase K was washed clean with HBSS for 3 times, and the sections were incubated with 3% H_2O_2 in PBS at room temperature for 20 min to inactivate the endogenous peroxidase. 50 μL of TUNEL assay buffer was added to the specimens and incubated in a dark place at 37°C for 60 min. The sections were washed once with HBSS, and added dropwise with 0.1-0.3 mL of stop buffer, followed by incubation at room temperature for 10 min. 0.2-0.5 mL of diaminobenzidine (DAB) developing solution was added dropwise, followed by incubation at room temperature for 5 min. Finally, the sections were observed under the microscope, and the apoptotic cells were counted.

Statistical Analysis

All data were expressed as mean ± standard deviation. The *t*-test was used for analyzing measurement data. Differences between the

two groups were analyzed using the Student's *t*-test. Comparison between multiple groups was made using One-way ANOVA test followed by Post-Hoc Test (Least Significant Difference). $p<0.05$ suggested the statistically significant differences.

Results

HE Staining

In group B, there was no significant damage to the structure of spinal cord tissues. In group C, the spinal cord tissues had disordered structure and significant fragmentation, the damage to grey matter was the greatest. Also, almost all of the grey matter was destroyed and dissolved, with a large number of scars and cavitation, and it was hard to distinguish between gray matter and white matter. In group A, the spinal cord tissues had a clear structure; there were smaller necrotic cavitation regions in the grey-white matter, and the number of cavitation significantly declined compared with that in group C (Figure 1).

Difference in GFAP Expression in the Injury Area Detected Via Immunofluorescence Assay

The results of immunofluorescence assay revealed that the expression of GFAP in spinal cord tissues was the lowest in group B, while it was markedly decreased in group A compared with that in group C ($p<0.05$), suggesting that injecting UCMSCs *via* the caudal vein can significantly reduce the expression of GFAP in spinal cord tissues (Figure 2).

Spinal Cord Neuronal Apoptosis Detected Via TUNEL Assay

According to the results of TUNEL assay, the spinal cord neuronal apoptosis rate was (4.21±0.19), (0.72±0.21) and (4.57±0.31), respectively, in group A, group B, and group C. It can be seen that the spinal cord neuronal apoptosis rate significantly declined in group A due to the treatment with UCMSCs, showing a significant difference compared with that in group C ($p<0.05$) (Figure 3).

P-p38 Protein Expression Level Detected Via Western Blotting

According to the results of Western blotting, the protein expression of p-p38 in spinal cord tissues was remarkably decreased in group B compared with that in group A and group C ($p<0.05$). Also, p-p38 protein expression was notably decreased in group A compared with that in group C ($p<0.05$), indicating that injecting UCMSCs *via* the caudal vein can significantly lower the protein expression of p-p38 in spinal cord tissues (Figure 4).

Discussion

The morbidity rate of SCI, a common central nervous system disease, has increased year by year[12,13]. MSCs are a kind of stem cells with differentiation ability. Also, stem cell transplantation is a potential therapeutic method for SCI[14]. One of the barriers to nerve regeneration after SCI is the glial scar, and the proliferation and hypertrophy of astrocytes are often accompanied by the up-regulation of the GFAP expression[10,15]. The expression of p38 MAPK, a protease closely related to in-

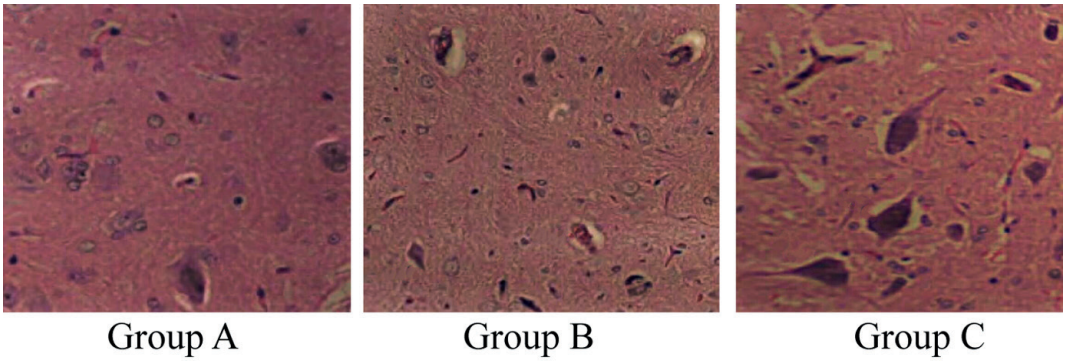

Figure 1. Observation of morphology of spinal cord tissues in the three groups (× 200).

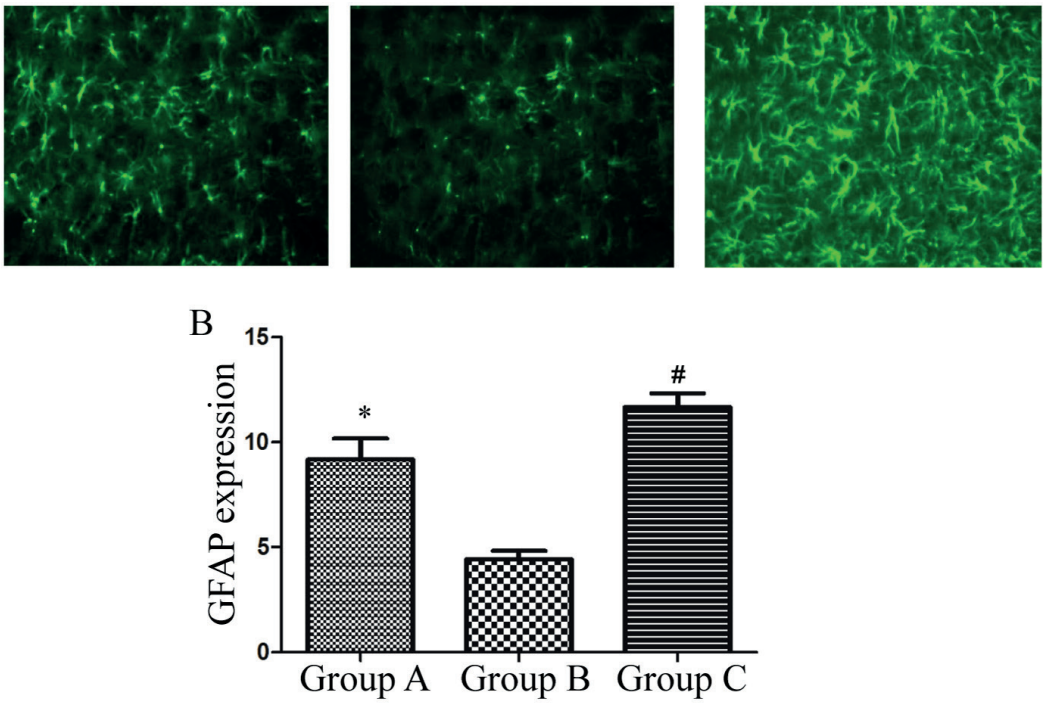

Figure 2. GFAP expression in the injury area in the three groups. ***A,*** Fluorescence diagram of GFAP expression (× 40), ***B,*** expression level of GFAP, **p*<0.05 *vs.* group C, #*p*<0.05 *vs.* group B.

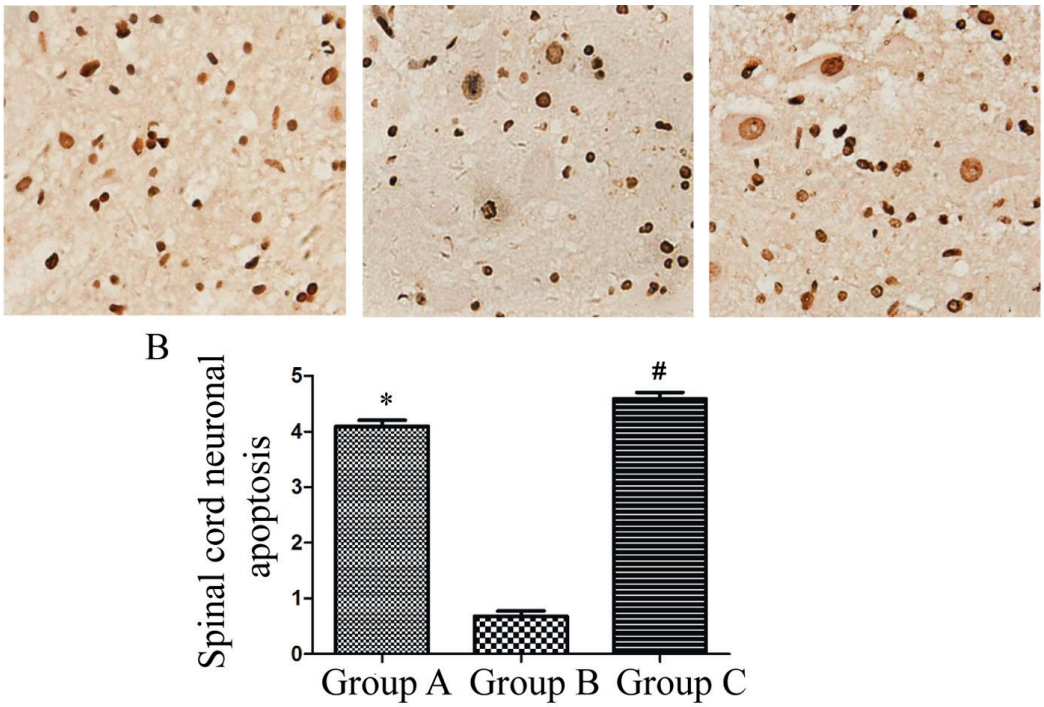

Figure 3. Spinal cord neuronal apoptosis. ***A,*** Spinal cord neuronal apoptosis detected *via* TUNEL assay (× 100), ***B,*** comparison of spinal cord neuronal apoptosis among groups. **p*<0.05 *vs.* group C, #*p*<0.05 *vs.* group B.

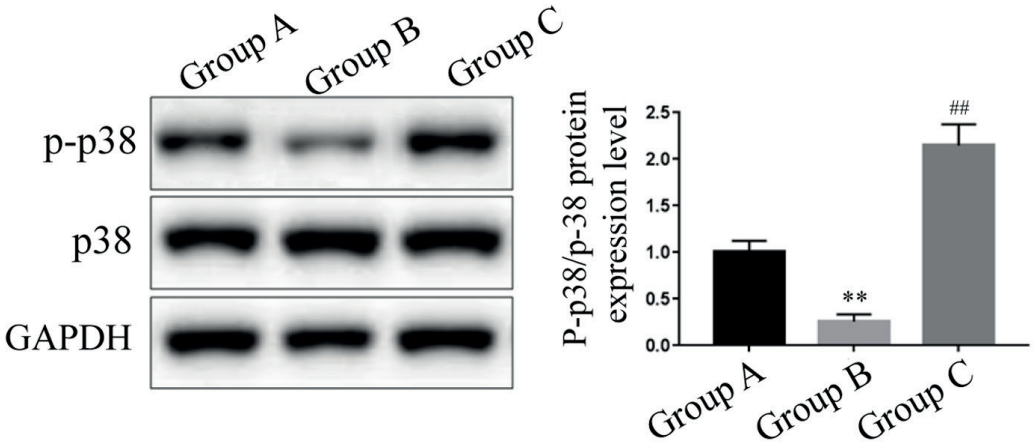

Figure 4. P-p38 protein expression level detected *via* Western blotting. **p<0.01 *vs.* group C, &&p<0.01 *vs.* group A.

flammatory response, will affect GFAP[16,17]. In the present work, the SCI model was established for experimental analysis. The results of HE staining showed that compared with group B, there were syringomyelia and excessively sparse nerve fibers in group A, as well as more syringomyelia and highly sparse nerve fibers with incomplete tissue structure in group C. The degree of syringomyelia and morphology and arrangement of nerve fibers in group A were superior to those in group C (p<0.05). Moreover, the results of immunofluorescence assay revealed that the expression of GFAP was the lowest in group B, while it was significantly decreased in group A compared with that in group C (p<0.05). Some reports[18,19] show that the main barrier to nerve regeneration in SCI is GFAP, while proliferation and hypertrophy of astrocytes after SCI inhibit the recovery of spinal cord nerve function, aggravating the condition of disease, consistent with the results in this paper.

The spinal cord neuronal apoptosis was detected *via* TUNEL assay. The spinal cord neuronal apoptosis rate was (4.21±0.19), (0.72±0.21), and (4.57±0.31), respectively, in group A, group B, and group C. It can be seen that the spinal cord neuronal apoptosis rate markedly declined in group A due to the treatment with UCMSCs. Also, there was a significant difference compared with that in group C, while it was significantly increased in group A compared with that in group B, but lower than group C (p<0.05). Some studies[20,21] have confirmed that UCMSCs isolated from human umbilical cord tissues have a certain effect on astrocytes; however, only the subculture can enable UCMSCs to suppress the excessive differentiation of astrocytes and raise the possibility of differentiation of UCMSCs into neuron-like cells[22,23]. The above findings indicate that UCMSCs can regulate the nerve injury and inhibit the neuronal apoptosis caused by SCI, consistent with the research results in this paper.

According to the results of Western blotting, the protein expression of p-p38 in spinal cord tissues was remarkably decreased in group B compared with that in group A and group C (p<0.05). Also, it was evidently decreased in group A compared with that in group C (p<0.05), indicating that injecting UCMSCs *via* the caudal vein can significantly lower the protein expression of p-p38 in spinal cord tissues.

Research[24] has confirmed that the p38MAPK expression will rise after SCI, and it is reported that after activation, p38 MAPK will transfer to the nucleus to act on other targets, accept stress signals for proliferation and differentiation in osteoblasts, and exert a regulatory function to enhance the activity of some transcription factors. A previous report[25] reveals that the decline in the p38 MAPK activity will inhibit the production of adipocytes, consistent with the results in this paper.

Conclusions

We showed that UCMSCs promoted the recovery of neurological function, inhibited the p38 MAPK pathway activated after SCI, and reduced the spinal cord neuronal apoptosis in SCI rats.

Conflict of Interests

The Authors declare that they have no conflict of interests.

References

1) Dong H, Li G, Shang C, Yin H, Luo Y, Meng H, Li X, Wang Y, Lin L, Zhao M. Umbilical cord mesenchymal stem cell (UC-MSC) transplantations for cerebral palsy. Am J Transl Res 2018; 10: 901-906.
2) Hao Y, Ran Y, Lu B, Li J, Zhang J, Feng C, Fang J, Ma R, Qiao Z, Dai X, Xiong W, Liu J, Zhou Q, Hao J, Li R, Dai J. Therapeutic effects of human umbilical cord-derived mesenchymal stem cells on canine radiation-induced lung injury. Int J Radiat Oncol Biol Phys 2018; 102: 407-416.
3) Sun Y, Wang Y, Zhou L, Zou Y, Huang G, Gao G, Ting S, Lei X, Ding X. Spheroid-cultured human umbilical cord-derived mesenchymal stem cells attenuate hepatic ischemia-reperfusion injury in rats. Sci Rep 2018; 8: 2518.
4) Song HL, Zhang X, Wang WZ, Liu RH, Zhao K, Liu MY, Gong WM, Ning B. Neuroprotective mechanisms of rutin for spinal cord injury through anti-oxidation and anti-inflammation and inhibition of p38 mitogen activated protein kinase pathway. Neural Regen Res 2018; 13: 128-134.
5) Dalamagkas K, Tsintou M, Seifalian A, Seifalian AM. Translational regenerative therapies for chronic spinal cord injury. Int J Mol Sci 2018; 19. pii: E1776.
6) Min J, Feng Q, Liao W, Liang Y, Gong C, Li E, He W, Yuan R, Wu L. IFITM3 promotes hepatocellular carcinoma invasion and metastasis by regulating MMP9 through p38/MAPK signaling. FEBS Open Bio 2018; 8: 1299-1311.
7) McKee C, Beeravolu N, Bakshi S, Thibodeau B, Wilson G, Perez-Cruet M, Rasul Chaudhry G. Cytotoxicity of radiocontrast dyes in human umbilical cord mesenchymal stem cells. Toxicol Appl Pharmacol 2018; 349: 72-82.
8) Huang L, Wang M, Yan Y, Gu W, Zhang X, Tan J, Sun H, Ji W, Chen Z. OX40L induces helper T cell differentiation during cell immunity of asthma through PI3K/AKT and P38 MAPK signaling pathway. J Transl Med 2018; 16: 74.
9) Hassan G, Bahjat M, Kasem I, Soukkarieh C, Aljamali M. Platelet lysate induces chondrogenic differentiation of umbilical cord-derived mesenchymal stem cells. Cell Mol Biol Lett 2018; 23: 11.
10) Kasuya Y, Umezawa H, Hatano M. Stress-activated protein kinases in spinal cord injury: focus on roles of p38. Int J Mol Sci 2018; 19. pii: E867.
11) Ren R, Chen SD, Fan J, Zhang G, Li JB. MiRNA-138 regulates MLK3/JNK/MAPK pathway to protect BV-2 cells from H2O2-induced apoptosis. Bratisl Lek Listy 2018; 119: 284-288.
12) Jia L, Chen Y, Tian YH, Zhang G. MAPK pathway mediates the anti-oxidative effect of chicoric acid against cerebral ischemia-reperfusion injury in vivo. Exp Ther Med 2018; 15: 1640-1646.
13) Yamamoto S, Yamashina K, Ishikawa M, Gotoh M, Yagishita S, Iwasa K, Maruyama K, Murakami-Murofushi K, Yoshikawa K. Protective and therapeutic role of 2-carba-cyclic phosphatidic acid in demyelinating disease. J Neuroinflammation 2017; 14: 142.
14) Zhang T, Jiang K, Zhu X, Zhao G, Wu H, Deng G, Qiu C. MiR-433 inhibits breast cancer cell growth via the MAPK signaling pathway by targeting Rap1a. Int J Biol Sci 2018; 14: 622-632.
15) Cotticelli MG, Xia S, Kaur A, Lin D, Wang Y, Ruff E, Tobias JW, Wilson RB. Identification of p38 MAPK as a novel therapeutic target for Friedreich's ataxia. Sci Rep 2018; 8: 5007.
16) Goldsmith CS, Kim SM, Karunarathna N, Neuendorff N, Toussaint LG, Earnest DJ, Bell-Pedersen D. Inhibition of p38 MAPK activity leads to cell type-specific effects on the molecular circadian clock and time-dependent reduction of glioma cell invasiveness. BMC Cancer 2018; 18: 43.
17) Fang CX, Ma CM, Jiang L, Wang XM, Zhang N, Ma JN, Wu TH, Zhang ZH, Zhao GD, Zhao YD. p38 MAPK is crucial for Wnt1- and LiCl-induced epithelial mesenchymal transition. Curr Med Sci 2018; 38: 473-481.
18) Zhao Z, Guo F, Sun X, He Q, Dai Z, Chen X, Zhao Y, Wang J. BMP15 regulates AMH expression via the p38 MAPK pathway in granulosa cells from goat. Theriogenology 2018; 118: 72-79.
19) Zhu L, Yi X, Zhao J, Yuan Z, Wen L, Pozniak B, Obminska-Mrukowicz B, Tian Y, Tan Z, Wu J, Yi J. Betulinic acid attenuates dexamethasone-induced oxidative damage through the JNK-P38 MAPK signaling pathway in mice. Biomed Pharmacother 2018; 103: 499-508.
20) Feng M, Wang L, Chang S, Yuan P. Penehyclidine hydrochloride regulates mitochondrial dynamics and apoptosis through p38MAPK and JNK signal pathways and provides cardioprotection in rats with myocardial ischemia-reperfusion injury. Eur J Pharm Sci 2018; 121: 243-250.
21) Yang XX, Wong YH, Zhang Y, Zhang G, Qian PY. Exploring the regulatory role of nitric oxide (NO) and the NO-p38MAPK/cGMP pathway in larval settlement of the bryozoan Bugula neritina. Biofouling 2018; 34: 545-556.
22) Li J, Xu Y, Ren H, Zhu Y, Peng B, Cui L. Autoimmune GFAP astrocytopathy after viral encephalitis: a case report. Mult Scler Relat Disord 2018; 21: 84-87.
23) Luessi F, Engel S, Spreer A, Bittner S, Zipp F. GFAPα IgG-associated encephalitis upon daclizumab treatment of MS. Neurol Neuroimmunol Neuroinflamm 2018; 5: e481.
24) Gyengesi E, Liang H, Millington C, Sonego S, Sirijovski D, Gunawardena D, Dhananjayan K, Venigalla M, Niedermayer G, Münch G. Investigation into the effects of tenilsetam on markers of neuroinflammation in GFAP-IL6 mice. Pharm Res 2018; 35: 22.
25) Cai F, Wu F, Cao J, Chen X. MicroRNA-146b-3p regulates the development and progression of cerebral infarction with diabetes through RAF1/P38MAPK/COX-2 signaling pathway. Am J Transl Res 2018; 10: 618-628.